

The faint-end of the galaxy luminosity function in groups

R. E. González¹, M. Lares², D. G. Lambas², and C. Valotto²

¹ Departamento de Astronomía y Astrofísica, Pontificia Universidad Católica de Chile, Casilla 306, Santiago 22, Chile.

² Grupo de Investigaciones en Astronomía Teórica y Experimental (IATE), Observatorio Astronómico de Córdoba, UNC, and Consejo Nacional de Investigaciones Científicas y Tecnológicas. (CONICET), Argentina.

Received ?? 2005 / Accepted ?? 2005

Abstract. We compute the galaxy luminosity function in spectroscopically selected nearby groups and clusters. Our sample comprises 728 systems extracted from the third release of the Sloan Digital Sky Survey in the redshift range $0.03 < z < 0.06$ with virial mass range $10^{11} M_{\odot} < M_{vir} < 2 \times 10^{14} M_{\odot}$. In order to compute the galaxy luminosity function, we apply a statistical background subtraction method following usually adopted techniques. In the r band, the composite galaxy luminosity function shows a slope $\alpha = -1.3$ in the bright-end, and an upturn of the slope in the faint-end, $M_r \gtrsim -18 + 5 \log(h)$, to slopes $-1.9 < \alpha < -1.6$. We find that this feature is present also in the i, g and z bands, and for all explored group subsamples, irrespective of the group mass, number of members, integrated color or the presence of a hot intra-cluster gas associated to X-ray emission.

Key words. methods: statistical – galaxies: clusters: general – galaxies: luminosity function

1. Introduction

The luminosity function (LF) of galaxies is one of the fundamental statistical tools for describing global properties of galaxy populations. This is important since variations in the LF in different environments can provide clues to the different evolutionary processes of galaxies. The LF of galaxies within groups and clusters of galaxies is then a key property for understanding the role of the environment on galaxy formation and evolution. Differences in the field and cluster galaxy LF, or between groups with different properties, could provide statistical indicators of these environmental effects.

The field and cluster galaxy LF have been calculated with a very good accuracy at the bright-end (brighter than $M_r \sim -17$) in different spectroscopic surveys (Blanton et al. 2004; Madgwick et al. 2002; Norberg et al. 2002; de Lapparent et al. 2003; De Propris et al. 2003). The study of faint galaxies ($M_r > -17$) is always restricted to small samples given the difficulties of obtaining redshifts for large number of such objects. Differences between the field and cluster galaxy LF at the bright-end may be caused by the interaction of galaxies in different environments. Ram pressure stripping can inhibit star formation by exhausting the gas present in galaxies that move fast in the intergalactic medium of rich clusters. Similarly, galaxy harassment can produce significant changes in the star formation rate of galaxies. These effects are not expected to be important in poor clusters or groups, where the velocity dispersion is lower, and instead, effects such as mergers or tidal interactions can be dominant in these environments. Studies using semi-analytic galaxies from numerical simulations show a

strong dependence of the LF on environment (González et al. 2005). On the observational side, Croton et al. (2005) find a significant dependence of the LF on local galaxy density in the 2dF galaxy redshift survey. Similar results were derived by Garilli et al. (1999) showing a correlation between the galaxy LF and cluster density.

A straightforward determination of the galaxy LF faint-end in galaxy systems requires long observing times to obtain spectra of faint objects in homogeneous samples. Individual analysis of nearby clusters or of the Local Group of galaxies have been performed (Deady et al. 2002; Mateo 1998; Zucker et al. 2004; Trentham et al. 2005), with the disadvantage of a low number statistics. On the other hand, statistical methods that perform a background subtraction offer the possibility of analyzing large faint galaxy samples in clusters. Several previous studies have made use of this technique (Goto et al. 2002; Garilli et al. 1999; Paolillo et al. 2001; Popesso et al. 2004b; Valotto et al. 2004). In these works it is detected an excess of dwarf galaxies in the faint-end of the LF so that a single Schechter function cannot provide an accurate fit to the data (Madgwick et al. 2002).

The large scale distribution of matter in the local universe can give rise to spurious clumps of galaxies when observed in projection. In fact, Valotto et al. (2001), using a deep mock catalogue constructed from a numerical simulation of a hierarchical universe, showed that a biased steep determination of the faint-end slope may be originated by projection effects of foreground/background structures. These effects induce a systematic bias that cannot be corrected by subtracting background fields.

Such systematic effects could be overcome if clusters are identified by X-ray detection or redshift space selection, assuring the presence of overdense regions without significant contamination along the line of sight. X-ray selected clusters may provide unbiased samples suitable for determining the galaxy LF by a statistical background subtraction method, since the hot gas confined in the gravitational potential well, responsible of the observed thermal bremsstrahlung emission in the X-ray band, is a reliable indicator of massive clusters. Popesso et al. (2004b), based on a sample of clusters with strong X-Ray emission (Popesso et al. 2004a) calculated the composite galaxy LF of RASS-SDSS clusters using statistical background subtraction methods and found a steep faint-end slope $\alpha \simeq -2$ which strongly supports the presence of a population of faint galaxies associated to rich clusters.

Popesso et al. (2004b) results correspond to galaxies within a dense intra-cluster medium, so it is of interest to extend this analysis to systems without strong X-ray emission. Clusters and groups of galaxies selected from spectroscopic surveys are also expected to be free from systematic identification biases as those present in two dimensional surveys and are ideal for this extension.

The large group and cluster sample obtained from the SDSS-DR3 spectroscopic survey by Merchán & Zandivarez (2005, hereafter MZ05) is suitable to calculate a reliable composite galaxy LF in galaxy systems of a wide range of virial masses extending previous results in rich clusters to more common galaxy environments. The size of this sample allows to analyze subsamples with different group properties (e.g., mass, sizes, color, morphology), so that the LF dependence on group characteristics can be assessed.

In this paper we study the galaxy LF in groups and clusters from MZ05, using a statistical background subtraction method from SDSS photometric data. We derive a reliable galaxy LF down to $M_r \simeq -14$ and explore different subsamples according to group and galaxy properties. The paper is structured as follows. In section 2 we describe the data used to calculate the composite LF in clusters. In section 3 we describe the method of statistical background subtraction adopted and the fitting functions. In section 4 we show the results for different subsamples in order to test for a possible dependence of the LF with group properties, we also compare our results with other studies in the field and in clusters. Finally, in section 5 we summarize our conclusions. Distance-dependent quantities are calculated using a Hubble parameter $H_0 = 100 h \text{ Km s}^{-1} \text{ Mpc}^{-1}$.

2. The data

In this paper we use the Third Data Release of the Sloan Digital Sky Survey (SDSS DR3, Abazajian et al. 2004), in fields centred in MZ05 groups and clusters. SDSS provides images and spectroscopic CCD data at high galactic latitudes, using a dedicated wide-field 2.5m telescope at Apache Point Observatory in South-East New Mexico. This survey includes imaging data in five bands over 5282 deg^2 , within a photometric and astrometric catalogue of 141 million objects. The photometric data were also taken from the SDSS DR3. We extracted circular shape fields centred in each group, subtending a projected radius of

$1.2 h^{-1} \text{ Mpc}$ at the group euclidean distance. The fields include galaxies in the five photometric bands with a 95% completeness at $u, g, r, i, z = 22.0, 22.2, 22.2, 21.3$ and 20.5 .

The galaxy groups used were taken from the galaxy group sample constructed by MZ05. In order to identify groups of galaxies in the SDSS DR3, they developed an algorithm based on the friends-of-friends percolation method of Huchra & Geller (1982). The groups have an overdensity threshold of $\delta\rho/\rho = 80$ and a line-of-sight linking length parameter $V_0 = 200 \text{ Km s}^{-1}$. The identification takes into account the variation of the number density of galaxies due to the apparent magnitude limit and the sky coverage of the galaxy catalogue. Also, the authors apply an iterative method in dense regions in order to turn artificial systems aside and achieve a better determination of the group centers (Díaz et al. 2005). The final sample of MZ05 comprises 10864 groups with at least four members. We used a fraction of these systems, confining the sample to the nearby groups with $0.03 < z < 0.06$ and whose corresponding SDSS fields lack evident incompleteness.

The redshift restriction was adopted to have a fair sample of groups for the following reasons: Although the linking length parameters used in the identification have been tested in mock catalogues, groups at too low redshift ($z < 0.03$) have an important contribution from peculiar velocities, and also, fields corresponding to these groups cover very large areas. In order to reach the faint-end of the galaxy LF, we adopted an upper redshift limit $z = 0.06$, that corresponds to an absolute magnitude $M_r = -14.08$ at the limiting apparent magnitude $m_r = 22.2$. From the total sample of MZ05 groups, the redshift restriction give us a subsample of 1782 systems. We have further removed groups which are affected either by mask-related completeness problems, or by large fluctuations in the number counts of galaxies in neighbouring regions surrounding the group centers. This conservative restriction provides 728 groups which are best suited for a reliable statistical background subtraction method and will be used hereafter.

We have also searched for X-ray counterparts of our groups in the RASS-SDSS catalogue using a simple criterion of proximity to associate MZ05 systems to RASS X-ray clusters. The RASS-SDSS is a compendium of X-ray emitting clusters of galaxies based on the ROSAT All Sky Survey (RASS) and the SDSS (Popesso et al. 2004a). Adopting a maximum allowed separation between a MZ05 groups and a RASS-SDSS objects of 0.5Mpc, all the RASS clusters within our redshift interval are matched by one MZ05 group belonging to our sample, resulting 15 clusters in common.

In order to characterize the environment of the groups, we used the virial mass and the number of members to define appropriate subsamples. We also defined two additional parameters that may be useful to characterize the environment of each group: the integrated color index and the dominant galaxy estimator.

The integrated color index of each group was calculated by integrating the luminosity of each spectroscopic member

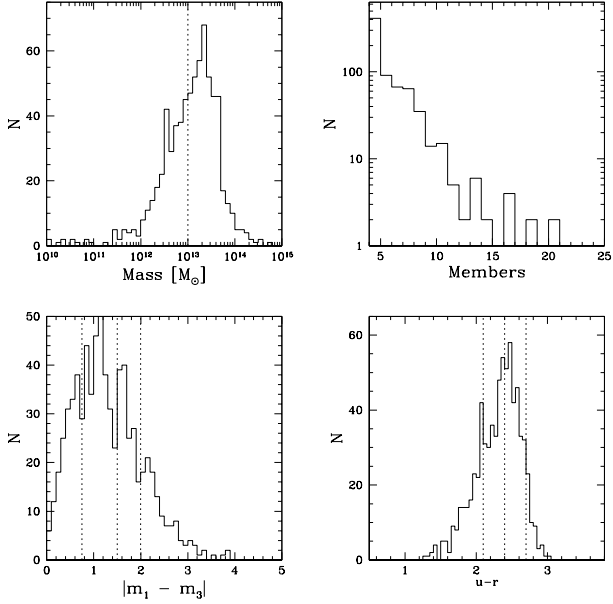


Fig. 1. Main properties of the 728 groups of the sample of groups. Top panels: Distribution of virial mass and number of spectroscopic members. Bottom panels: Distribution of dominant galaxy estimator and integrated color index. Dotted lines represent cuts of the sample for further analysis.

galaxy in the u and r bands, L_u and L_r respectively, and obtaining a global color of the group, according to:

$$u - r = -2.5 \text{Log} \left[\frac{\sum L_u}{\sum L_r} \right]. \quad (1)$$

The dominant galaxy estimator is defined by the usual criterion of the difference between the magnitudes of the brightest and the third-ranked member of each group, $|M_{r1} - M_{r3}|$.

Figure 1 shows the distribution of the main properties of our total sample of 728 groups. The dashed lines correspond to the different cuts adopted.

3. Background estimation and Luminosity Function computation.

Our study of the galaxy LF is based on a statistical background subtraction method applied in order to statistically remove the contribution of foreground and background galaxies in the fields of MZ05 groups. Local variations in the background number density of galaxies can be taken into account by using a local rather a global background, close enough to consider these local variations, but beyond the group region. Taking into account these considerations, we derived a local background using galaxies in a ring $2 h^{-1} \text{Mpc} < R_p < 5 h^{-1} \text{Mpc}$ centred in each group. We find that the results of using either local or global statistical background subtraction methods are consistent with each other within the rms scatter of each magnitude bin. However, the advantage of a global background relies in the fact that it can be very stable statistically if derived from a

sufficiently large area. Therefore we adopted this global background to perform the statistical decontamination in the group fields. The steps followed to decontaminate the galaxy counts are: 1- We selected 4816 random fields within the area covered by the spectroscopic SDSS DR3. Each field has an angular radius 8 arcmin so that the total number of fields comprise $\sim 3.6 \times 10^6$ galaxies in an area of 268.97 square degrees. 2- From these fields, we constructed a distribution of apparent magnitudes binned in 0.25 mag intervals. 3- For each group we subtracted this background distribution normalized to the relative area of the group region and the background. This procedure was applied to three regions centred in each group defined by $R_p < 0.3 h^{-1} \text{Mpc}$, $R_p < 0.5 h^{-1} \text{Mpc}$, $R_p < 0.7 h^{-1} \text{Mpc}$ and $0.3 < R_p < 0.7 h^{-1} \text{Mpc}$. 4- We summed the excess in the number of galaxies for each group in each apparent magnitude interval. We assume that the excess galaxies are at the mean group redshift so that for each group we obtain an absolute magnitude distribution. 5- We defined different subsamples according to group properties, as discussed in section 4, and summed the contributions to the galaxy LF of each group of the subsamples. We have considered an apparent limiting magnitude $r = 22.2$ corresponding to a 95% completeness. At the maximum redshift of our sample of groups, $z < 0.06$, this corresponds to an absolute limiting magnitude $M_r = -14.25$. Absolute magnitudes were computed using $M = m - 25 - 5 \log_{10}(D_L)$, where D_L is the luminosity distance in Mpc . Due to the low redshift of the sample, K-corrections are negligible.

Since it is observed an upturn in the galaxy LF derived we adopted two different Schechter functions (Schechter 1976) for the bright and the faint region respectively (see next section for details):

$$\phi(M) dM = 0.4 \ln(10) \phi^* e^{-X} X^{\alpha+1} dM$$

where $X = 10^{0.4(M^* - M)}$, the parameter M^* refers to the characteristic luminosity; α is the faint-end slope indicating the relative importance of a population of low luminosity galaxies, and ϕ^* is the LF normalization. Using a maximum likelihood estimator we fit the best Schechter functions in both the bright and in faint region of the LF. In tables 1 and 2 we show fits for different subsamples of our data. Errors on these tables correspond to 1σ contours (68% confidence), following Poisson statistics in the galaxy counts.

4. Analysis and results

We have typically $\approx 8000 - 12000$ galaxies per square degree in each group field, brighter than $m_r = 22.2$, out of which $\approx 100 - 4000$ are in excess within $0.7 h^{-1} \text{Mpc}$ with respect to the mean global background. This allows us to construct the distribution of absolute magnitudes, and use it to compute the galaxy LF. The results for the composite LF of our total sample of 728 groups is shown in figure 2, the faintest bin ($-14 < M_r < -14.25$) has a Poisson uncertainty less than 10%. In this figure we also show, with arbitrary normalization, Popesso et al. (2004b) results for galaxies in 97 clusters of the RASS-SDSS sample, and the field LF determination of Blanton et al. (2004). We can appreciate that the bright-ends are similar, and that X-ray clusters and optical groups also have

comparable steep faint-ends, with the LF of galaxies in groups slightly flatter than that of galaxies in the X-ray selected sample. We notice that although MZ05 groups and X-ray clusters in Popesso et al. (2004b) may differ considerably in their properties, the galaxy LF are remarkably similar, indicating that a rising LF at the faint end is a generic feature of galaxy systems. A single Schechter function does not provide an accurate fit to the observed galaxy LF due to this upturn occurring approximately at $M_r = -18$. Two separate Schechter functions provide an appropriate fit to both the bright and faint regions as can be appreciated in fig 2. By comparison of different determinations of the galaxy LF, it can be seen the presence of a statistically significant excess of extremely faint galaxies ($M_r > -17.$) in our analysis and in Popesso et al. (2004b), with respect to the field galaxy LF obtained by Blanton et al. (2004). We notice, however, the lack of faint galaxies in the spectroscopic surveys so that the faint-end slope in the field can be strongly affected by completeness corrections. The agreement of our composite LF with Blanton et al. (2004) determination at intermediate magnitudes and in the bright-end where there is a reasonable completeness in Blanton et al. (2004) provides confidence in our statistical background subtraction procedure. We have assessed the reliability of the faint-end slope determination taking into account the Poisson uncertainty of the global background fluctuation $\sim 1\%$ and the fact that we achieve $\sim 95\%$ completeness in the faintest magnitude bins. It would be required a relative error as large as 40% in order to make our faint end determination consistent with Blanton et al. (2004).

We have also derived the composite galaxy LF in the other SDSS photometric bands (u, g, i, z). The results are shown in figure 3, and in table 1 we list the two component Schechter function fits to each LF, with upturn limits in $M_g, M_i, M_z = -17.5, -18.5$ and -19 . Therefore, the galaxy LF requires two Schechter functions to provide a suitable fit to the observations, except for the u -band where we can only see the bright-end. For this band, we would expect the upturn close to the magnitude limit, since the mean color $u - r \simeq 2.4$ of groups would imply an upturn at $M_u \simeq -15.6$. Photometric errors are small in the g, r and i band, where the upturn of the LF is clear; in u and z -bands photometric errors are greater and the completeness limit is $\simeq 0.5$ magnitudes brighter, although the upturn in the z -band is clear. This is consistent with a constant extent of the bright region of ~ 4.5 magnitudes in all bands. In order to explore a possible dependence of the dwarf galaxy population on group-centric distance, we consider the counts of galaxies for each galaxy group in four regions, $0 < R_p < 0.3 h^{-1} Mpc$, $0 < R_p < 0.7 h^{-1} Mpc$, $0.3 < R_p < 0.7 h^{-1} Mpc$. These results are shown in figure 4 and in table 2 where it can be appreciated that the faint-end slope is steeper in the outskirts of clusters, where a larger fraction of star-forming galaxies is expected by the morphological segregation of galaxies in clusters (Andreon 1996; Domínguez et al. 2002). Although with a lower statistical significance, bright galaxies are found to be more strongly concentrated.

band	α_{bright}	M_{bright}^*	α_{faint}	M_{faint}^*	ϕ_b^*/ϕ_f^*
u	-0.79 ± 0.06	-17.68 ± 0.05	-1.12 ± 0.15	-17.67 ± 0.4	1.3913
g	-1.12 ± 0.06	-20.10 ± 0.10	-1.67 ± 0.03	-21.95 ± 0.5	11.695
r	-1.31 ± 0.04	-21.42 ± 0.12	-1.89 ± 0.04	-21.94 ± 0.5	11.509
i	-1.18 ± 0.08	-21.50 ± 0.17	-1.74 ± 0.03	-21.97 ± 0.5	6.4023
z	-1.14 ± 0.05	-21.91 ± 0.15	-1.64 ± 0.10	-21.85 ± 0.6	3.8122

Table 1. Galaxy LF bright and faint-end Schechter fits parameters in the five photometric bands within $0.5 h^{-1} Mpc$ of group-centric distance.

4.1. Galaxy LF dependence on group properties

We have explored several subsamples of groups according to the number of members, and total virial mass. We have also considered two additional parameters described in section 2, the group integrated color index and the dominant galaxy contrast parameter. By studying the galaxy LF in subsamples according to different ranges in the number of members, we conclude that there are no important differences in the results although we detect that in the richer systems the galaxy LF has a slightly flatter faint-end slope as we can see in figure 5. The results of the composite LF for groups of different virial mass can be appreciated in figure 6 and table 2 where it can be seen that there are no substantial differences between high and low group mass, although here again there is a trend for massive groups to have a flatter LF faint-end slope. This result is consistent with the fact that the galaxy LF in groups and in rich, X-ray emitting clusters are similar.

In order to explore the presence of possible evolution effects, we have divided the group sample according to both the group integrated color index and the dominant galaxy estimator using spectroscopic members, without imposing no further restrictions on the other group parameters. By comparing the results for subsamples defined by extreme values of these parameters, we aim to find possible differences in the galaxy LF as a result of evolution in groups. According to our analysis, no relevant differences are obtained. By inspection to figures 8 and 7, and table 2, it can be appreciated the lack of significant differences in the global shape of the galaxy luminosity function regardless of the parameter of the subsample analyzed. The results indicate that irrespective of the integrated color index, or the presence of a dominant galaxy, groups have a similar galaxy LF. Our findings support the existence of a similar large fraction of dwarf galaxies, regardless of mass, average color, or dominant galaxy luminosity contrast of the groups.

Finally, we plot in 9 the composite galaxy LF for the subsample of 15 X-ray emitting systems described in section 2. It can be seen in this figure that irrespective of the presence of a hot intra-group gas, the galaxy LF faint-end slopes of rich groups are similar. By inspection to table 2 it can be appreciated that the faint-end slope $\alpha = -1.68 \pm 0.10$ for the 15 groups coincident with the RASS-SDSS sample is consistent with $\alpha = -1.78 \pm 0.06$ derived for rich groups with more than 10 members.

Dataset	α_{bright}	M_{bright}^*	α_{faint}	M_{faint}^*	ϕ_b^*/ϕ_f^*
Background Subtraction					
in total sample	-1.31±0.04	-21.40±0.12	-1.89±0.04	-21.94±0.5	11.509
Group centric distance [h^{-1} Mpc]					
0.3	-1.14±0.03	-21.2 ± 0.2	-1.80±0.03	-21.42±0.7	10.759
0.7	-1.44±0.04	-21.7 ± 0.2	-1.96±0.03	-21.52±0.8	5.7132
0.3-0.7	-1.58±0.05	-21.76±0.25	-1.99±0.03	-20.98±0.7	1.869
Members					
4 to 6	-1.39±0.08	-21.72±0.20	-1.90±0.08	-21.70±0.6	6.2556
6 or more	-1.30±0.06	-21.35±0.15	-1.85±0.03	-21.80±0.7	9.5694
10 or more	-1.31±0.08	-21.22±0.20	-1.78±0.06	-21.95±0.8	9.9988
Mass [M_\odot]					
$10^{10} - 10^{13}$	-1.30±0.09	-21.52±0.25	-1.93±0.10	-21.30±0.8	7.7569
$10^{13} - 10^{15}$	-1.31±0.05	-21.35±0.20	-1.85±0.03	-21.77±0.6	8.2840
Integrated group Color u-r					
0.0 - 2.4	-1.32±0.08	-21.17±0.19	-1.89±0.07	-21.72±0.9	9.9962
2.4 - 4.0	-1.30±0.06	-21.62±0.20	-1.87±0.04	-21.65±0.9	7.8454
0.0 - 2.1	-1.16±0.13	-20.10±0.22	-1.86±0.40	-17.82±1.2	0.7694
2.7 - 4.0	-1.30±0.12	-21.95±0.21	-1.83±0.13	-19.05±1.4	0.6582
Dominant galaxy contrast [$M_{r1} - M_{r3}$]					
1.5 - 5	-1.33±0.03	-21.97±0.18	-1.87±0.06	-21.88±0.9	6.9975
0 - 1.5	-1.19±0.06	-20.98±0.13	-1.90±0.05	-21.97±1.2	18.992
0 - 0.75	-1.03±0.09	-20.63±0.15	-1.83±0.06	-21.87±0.5	16.856
2.0 - 5	-0.51±0.12	-21.17±0.17	-1.74±0.05	-21.82±0.6	9.5708
RASS-SDSS groups sample					
15 groups	-1.09±0.08	-20.75±0.14	-1.68±0.10	-20.57±1.4	4.4755

Table 2. r-band LF bright and faint regions Schechter fits for the different subsamples. Otherwise stated, the composite LF is determined within $0.5 h^{-1}$ Mpc.

5. Conclusions

We provide on firm statistical basis the presence of a steep faint-end in the galaxy LF in groups and poor clusters, with small variations according to group properties. The results are consistent with those obtained in X-ray clusters by Popesso et al. (2004b). The spurious detections of clumps in projection is an usual disadvantage of statistical background subtraction methods. We argue that this not introduce a significant bias when selecting the centers of the clusters in redshift space. We also notice that since the groups were selected in redshift space, they are not likely to be affected by the projection effects explored in Valotto et al. (2001). Our analysis is complete down to $M_r = -14.25$ and thus provide a reliable determination of the relative fraction of faint objects in galaxy systems. Overall, the shape of the galaxy LF cannot be described by a single Schechter function, mainly due to an upturn of the faint-end slope, occurring at $M_r \sim -18$. The observed faint-end slope is quite steep, $\alpha \simeq -1.9$ indicating a large fraction of faint galaxies in groups and clusters. This is consistent with Popesso et al. (2004b) results for X-ray clusters providing strong evidence that the upturn is not an exclusive feature of galaxies in a hot gas environment. Consistent with previous works, we also find evidence that the characteristic luminosity M^* is brighter in groups and clusters than in the field.

We have analyzed several subsamples of groups with different properties such as virial mass, number of members, global color index, and presence of a dominant galaxy. In all cases, we find only small variations of the shape of the LF in the faint-

end. This suggests a universal nature of the shape of the galaxy LF in galaxy system.

Acknowledgements. This work was supported by the Latin American-European Network on Astrophysics and Cosmology of the European Union's ALFA Programme, the Consejo Nacional de Investigaciones Científicas y Tecnológicas (CONICET), the Secretaría de Ciencia y Técnica (UNC), and the Agencia Córdoba Ciencia.

Funding for the creation and distribution of the SDSS Archive has been provided by the Alfred P. Sloan Foundation, the Participating Institutions, the National Aeronautics and Space Administration, the National Science Foundation, the U.S. Department of Energy, the Japanese Monbukagakusho, and the Max Planck Society. The SDSS Web site is <http://www.sdss.org>.

The SDSS is managed by the Astrophysical Research Consortium (ARC) for the Participating Institutions. The Participating Institutions are The University of Chicago, Fermilab, the Institute for Advanced Study, the Japan Participation Group, The Johns Hopkins University, the Korean Scientist Group, Los Alamos National Laboratory, the Max-Planck-Institute for Astronomy (MPIA), the Max-Planck-Institute for Astrophysics (MPA), New Mexico State University, University of Pittsburgh, Princeton University, the United States Naval Observatory, and the University of Washington.

References

- Abazajian, K., Adelman-McCarthy, J. K., Agüeros, M. A., et al. 2004, *AJ*, 128, 502
- Andreon, S. 1996, *A&A*, 314, 763
- Blanton, M., Lupton, R., Schlegel, D., et al. 2004, *ApJ*, submitted, astro-ph/0410164

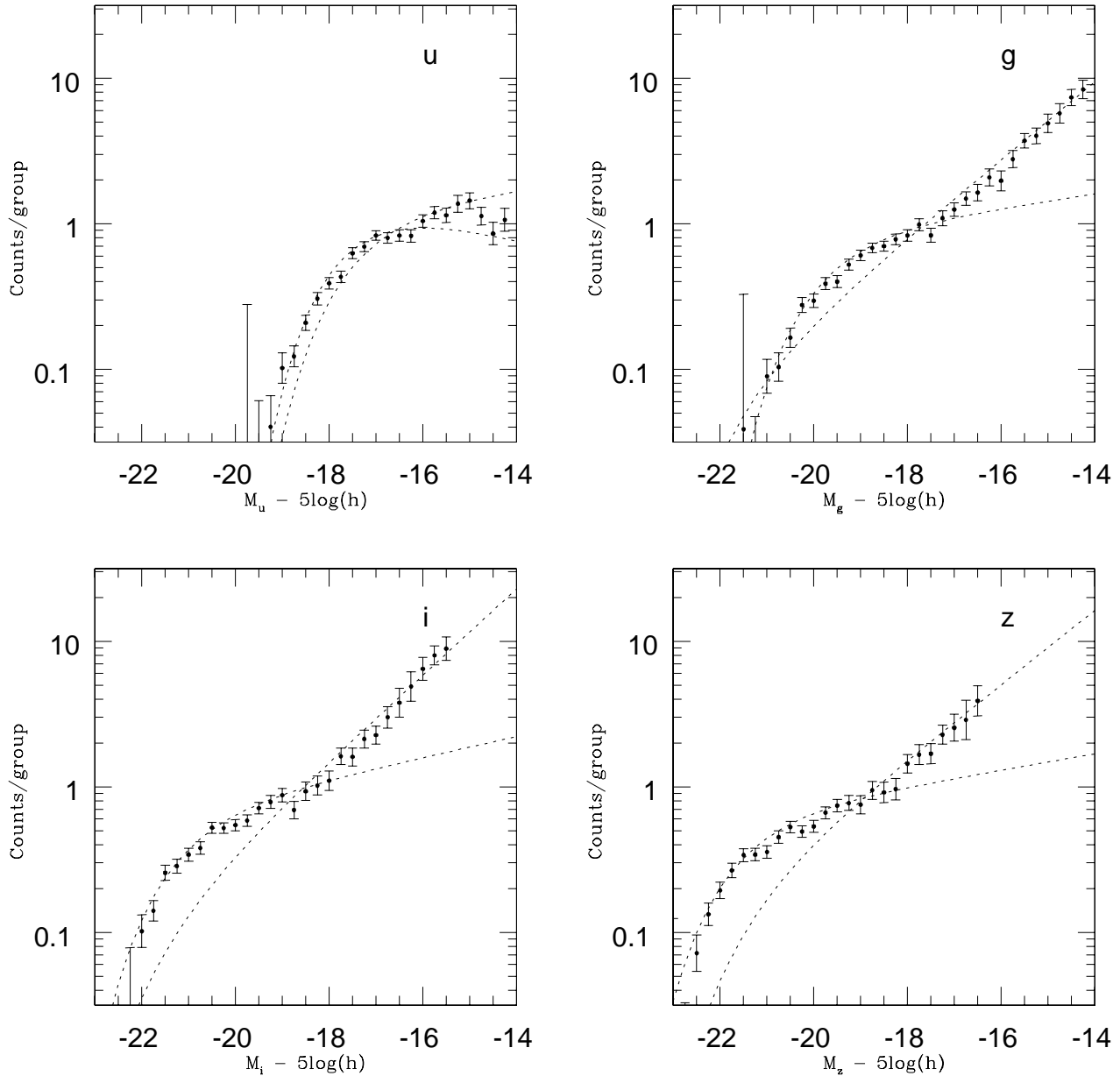


Fig. 3. Composite galaxy LF in the u, g, i, z photometric bands calculated for the total group sample within $0.5 h^{-1} Mpc$ from group centres.

Croton, D. J., Farrar, G. R., Norberg, P., et al. 2005, MNRAS, 356, 1155
 de Lapparent, V., Galaz, G., Bardelli, S., & Arnouts, S. 2003, A&A, 404, 831
 De Propris, R., Colless, M., Driver, S., et al. 2003, MNRAS, 342, 725
 Deady, J. H., Boyce, P. J., Phillipps, S., et al. 2002, MNRAS, 336, 851
 Díaz, E., Zandivarez, A., Merchán, M., & Muriel, H. 2005, ApJ submitted

Domínguez, M., Zandivarez, A., Martínez, H., et al. 2002, MNRAS, 335, 825
 Garilli, B., Maccagni, D., & Andreon, S. 1999, A&A, 342, 408
 González, R. E., Padilla, N., Galaz, G., & Infante, L. 2005, MNRAS, accepted, astro-ph/0508220
 Goto, T., Sekiguchi, M., Nichol, R. C., et al. 2002, AJ, 123, 1807
 Huchra, J. & Geller, M. 1982, ApJ, 257, 423
 Madgwick, D., Lahav, O., Baldry, I. Baugh, C. M., et al. 2002, MNRAS, 333, 133
 Mateo, M. L. 1998, ARA&A, 36, 435

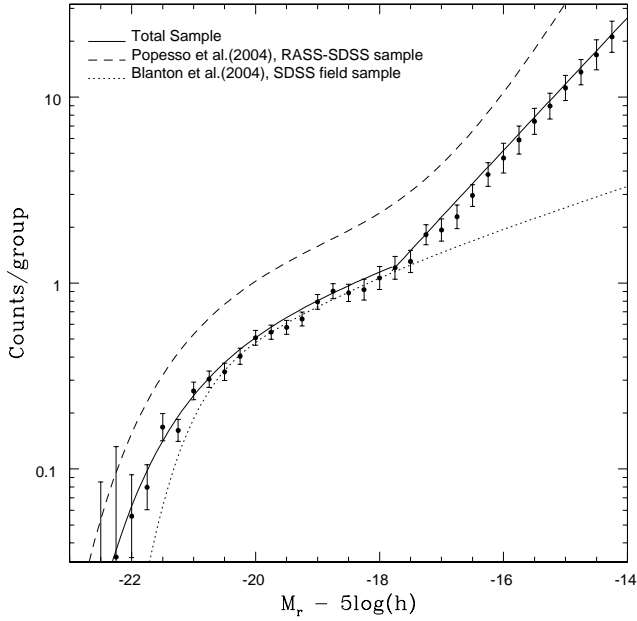


Fig. 2. r-band composite galaxy LF for the total sample of groups calculated within $0.5h^{-1}$ Mpc from group centres. The solid line corresponds to the best two Schechter function fits obtained from a maximum likelihood estimator with an upturn limit at $M_r = -18$ (see 4.1 for parameter values). For comparison we show with an arbitrary normalization Popesso et al. (2004b) and Blanton et al. (2004) LF determinations of galaxies in X-ray clusters and in the field, respectively.

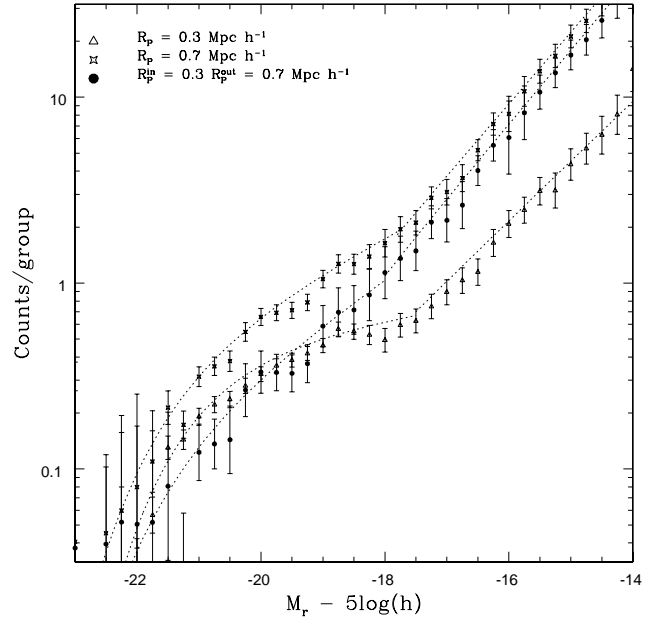


Fig. 4. Composite r-band galaxy LF for different group centric distance ranges.

Merchán, M. & Zandivarez, A. 2005, MNRAS, in press, astro-ph/0412257
 Norberg, P., Cole, S., Baugh, C. M., et al. 2002, MNRAS, 336, 907
 Paolillo, M., Andreon, S., Longo, G., et al. 2001, A&A, 367, 59
 Popesso, P., Böhringer, H., Brinkmann, J., et al. 2004a, A&A, 423, 449
 Popesso, P., Böhringer, H., M., R., & W., V. 2004b, A&A, in press, astro-ph/0410011
 Schechter, P. 1976, ApJ, 203, 297
 Trentham, N., Sampson, L., & Banerji, M. 2005, MNRAS, 357, 783
 Valotto, C., Moore, B., & Lambas, D. G. 2001, ApJ, 546, 157
 Valotto, C., Muriel, H., Moore, B., & Lambas, D. G. 2004, ApJ, 603, 67
 Zucker, D. B., Kniazev, A. Y., Bell, E. F., et al. 2004, ApJ, 612, 121

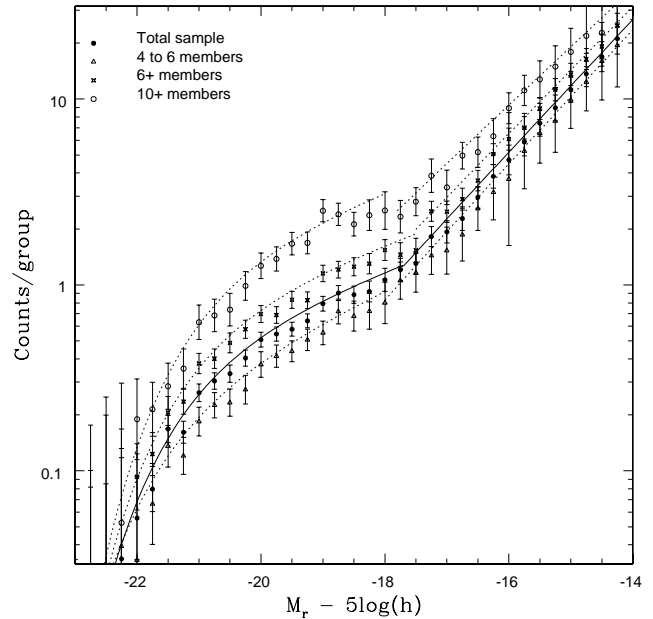


Fig. 5. Dependence of the composite galaxy LF, on the number of group members. It can be appreciated that the faint-end slope is slightly flatter for groups with more members.

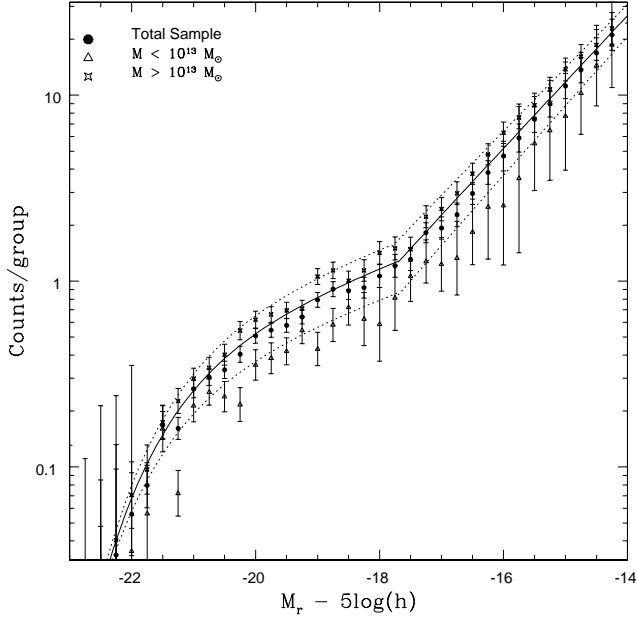


Fig. 6. Composite galaxy LF for different group mass ranges.

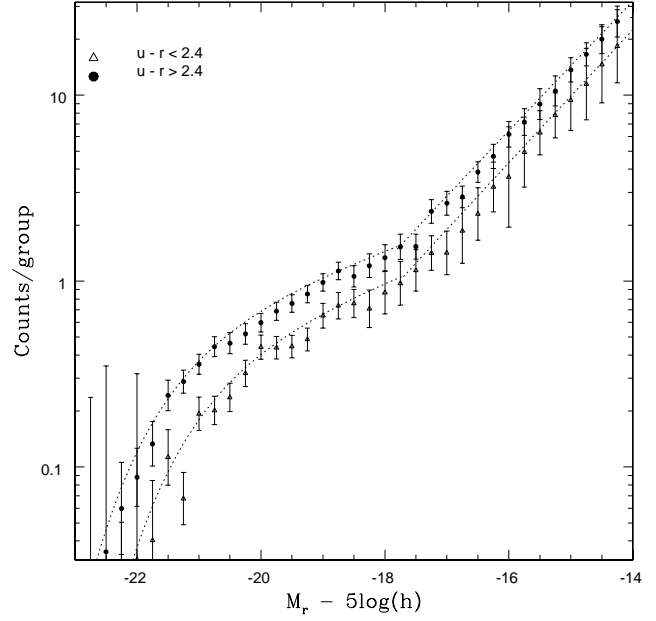


Fig. 8. Composite galaxy LF for groups with different ranges of integrated color index.

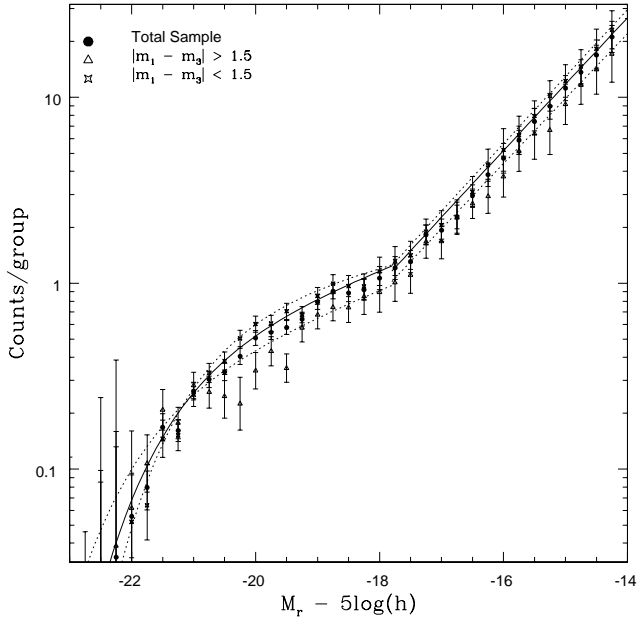


Fig. 7. Composite galaxy LF for groups with different dominant galaxy estimator.

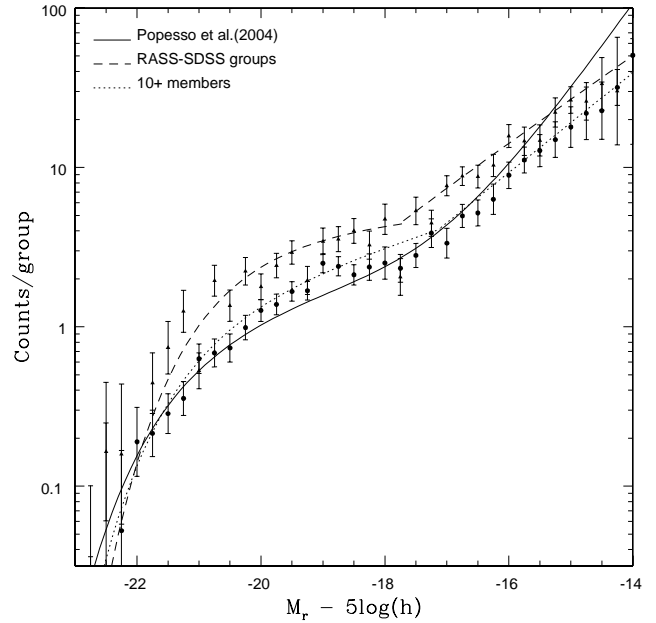


Fig. 9. r-band composite galaxy LF of the 15 RASS-SDSS clusters in our sample. For comparison we plot the composite galaxy LF of the groups with more than 10 members, and with an arbitrary normalization, the galaxy LF of the full RASS-SDSS sample determined by Popesso et al. (2004b).